Interannual Variability in Daily Characteristics of Winter Precipitation at Tallahassee, 1949 - 2016

Holli Capps

School of Natural Resources and the Environment,
College of Agricultural and Life Science,
University of Florida

Contact: Hcapps65@ufl.edu

Abstract

Knowledge of the risks, or variability, associated with daily precipitation characteristics: their frequency, magnitude and duration, is fundamental to correct management and planning of many human activities. Characterization of current interannual variability is crucial when predicting how different factors like agricultural production, forest-fire risks and streamflow (high and low) might adapt/react to climate change. Such predictions are informed by inputs from models called weather generators, which include a section on daily precipitation.

This research examines the parameters employed by weather generators (probabilities of wet-to-wet and dry-to-dry transitions, and mean and variance of daily precipitation) during winter at Tallahassee, which possesses a long and near-complete daily record. Winter precipitation in the Panhandle of Florida constitutes a greater proportion of annual total than much of Florida and falls when more is directed to land-based hydrologic stores. Winter is also when El Niño-Southern Oscillation (ENSO) has a pronounced regional impact with higher seasonal totals during warm phases (El Niño) and lower during cold (La Niña).

How the properties of daily precipitation respond to ENSO is investigated through the combined use of probability distributions, standard parametric tests and the non-parametric hypergeometric distribution. Higher seasonal totals in warm phases result from more frequent days with precipitation (but no significant changes in transition probabilities) and higher mean and variance of totals. Cold phases are more prone to less frequent events, particularly lower wet-to-wet transitions, and lower means and variances of daily total.

Keywords

Precipitation, variability, interannual, precipitation characteristics, winter, Panhandle, Tallahassee Florida

Introduction

The success of agriculture and many other human endeavors depends greatly on the vagaries of daily precipitation characteristics. In the absence of artificial impoundments or access to wells, a sequence of dry days without precipitation at a particularly crucial time in the growing season can have devastating consequences. Likewise, excessive precipitation can cause soil erosion and the loss of seeds and young plants, while a sequence of wet days at the time of harvest can damage crops and prevent removal. Variability in climate and associated weather is a major source of risk not only to agricultural productivity (Jones, 1993), but also fires (Elliot et al., 2016), floods (Sunde et al., 2017), droughts (Herman et al., 2016), slope stability (Bovy et al., 2016), health (Sparks et al., 2018) and soil erosion (Kinnell, 2019). Concerns heighten with anticipated changes in extremes of wet and dry periods resulting from climate change. The largest causes of current climate variability globally is the El Niño-Southern Oscillation (ENSO), a coupled ocean-atmosphere phenomenon seated in the equatorial Pacific. There are multiple phases defined by an increase or decrease in sea surface temperatures and associated atmospheric circulation, originating in the equatorial Pacific Ocean every 3-7 years. Precipitation and other climatic variables are known to vary worldwide as result. (https://iridl.ldeo.columbia.edu/maproom/ENSO/ENSO_Info.html). Over the past three decades, the ability to forecast the likely phase of ENSO (warm, neutral or cold) six to nine months ahead has improved markedly. This research addresses whether forecasts at the hemispheric scale can be translated to risks of daily precipitation properties at the local scale. In particular, the long record of daily precipitation at Tallahassee, with its implications for the economy of rural northwest Florida, including agriculture, forestry, tourism and estuarine shellfisheries, is examined.

The properties of daily precipitation constitute an important element of statistical weather generators used to determine stochastic weather inputs to models of various biophysical processes (Wilks and Wilby, 1999). The approach to representing precipitation characteristics has to be probabilistic because of, 1) the inherent variability in weather, 2) the fact that no two years of ENSO phases are identical, and 3) the need for farmers and other agents to make their own evaluations of the balance between risks and potential profits. The two major questions asked simply break down into, "Was there measurable precipitation?", and, "If so, how much precipitation fell?"

Study area and data

The climate of Tallahassee is fairly typical of the panhandle of Florida and the meteorological station possesses a long, reliable record of daily precipitation (1949-2016), with few missing data points. Data are available from the Florida Climate Center http://climatecenter.fsu.edu/jumi/climate_visualization/Climate_Data.php. The importance of winter precipitation is a distinguishing feature of the climate of the Florida panhandle. Between a quarter and a third of annual precipitation occurs in the winter, compared to peninsular Florida where this proportion drops to less than a fifth (Figure 1).

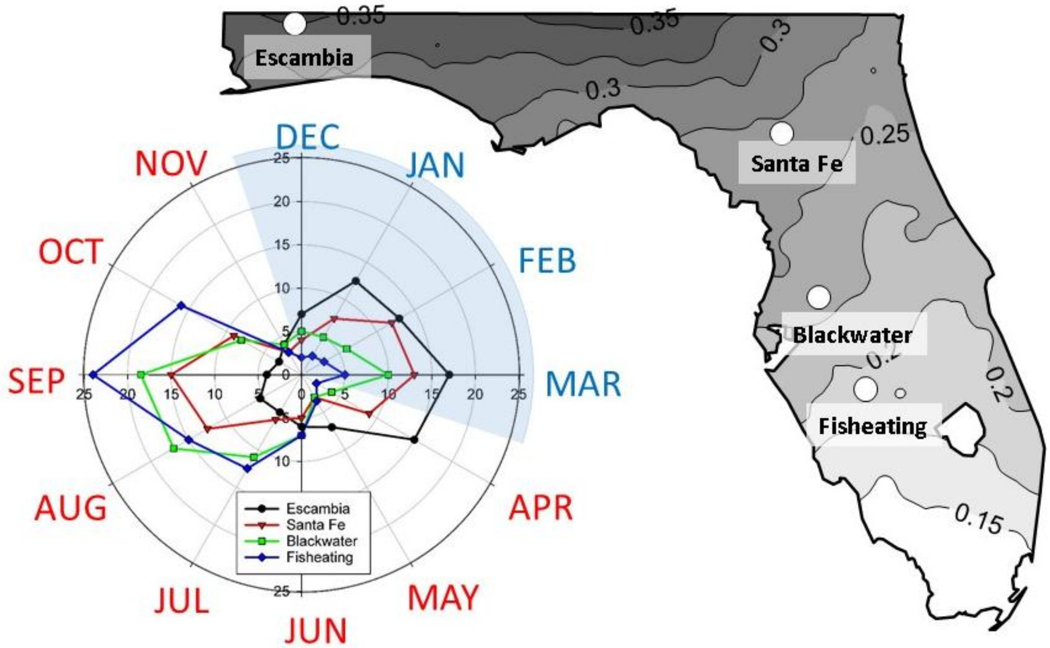

Figure 1. Polar plots of mean monthly runoffs expressed as percentages of the annual mean precipitation for four Florida rivers, from the Escambia (black) in the northwest, to Fisheating Creek (blue) in the south. Blue shading illustrates the winter wet season definition employed in this paper. Stations are located on a map displaying the proportion of mean annual precipitation falling in the months November-April.

Regional differences become more noticeable when viewed through the lens of monthly streamflow regimes of the four selected sites shown (Figure 1). Note the relative importance of winter flows in the north (Escambia and Santa Fe) compared to those flows in the south, and the intervening geographic gradient. Although the Escambia drains areas north of the Florida line where winter precipitation is more important, losses of precipitation to evapotranspiration are much lower than in summer, leaving a higher proportion of the precipitation to runoff as streamflow. Thus, winter events are of considerable impact upon available regional water resources.

During warm phases of ENSO (El Niño), winter precipitation totals increase, fed by a southerly displacement of the sub-tropical jet from the Pacific tracking storms across the region. During cold phases (La Niña) storm tracks and jets tend to move north of the area producing lower totals (Schmidt et al., 2001; Maleski and Martinez, 2018; Wang and Asefa, 2018). It is hypothesized that under future climate scenarios, the frequency of the warm and cold phases of ENSO will increase in frequency and intensity (Cai, et al., 2014, Cai et al., 2018.

For the sake of objectivity, years are classified *a priori* as warm, neutral or cold phases of ENSO according to the Center for Ocean-Atmospheric Prediction Studies (COAPS) at FSU, (https://www.coaps.fsu.edu/jma) based on definitions used by the Japanese Meteorological Association. Of the 63 years of complete record available, 16 are classified as warm phase ENSO, 30 as neutral and 17 as cold.

Weather generators seek to simulate the properties of both the sequences of wet and dry days, and daily total precipitation. The former property relates to the frequency of daily precipitation and the latter its magnitude.

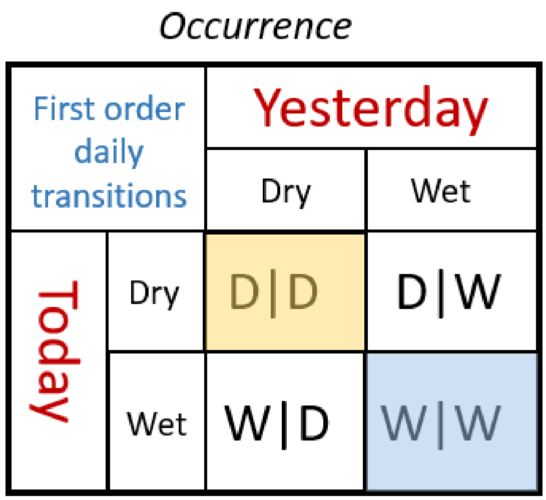

$$p(W|D) = 1-p(D|D)$$

$$p(D|W) = 1-p(W|W)$$

Figure 2. Possible combinations of two consecutive days with or without precipitation. Defining the occurrence of daily precipitation.

The sequence of wet and dry days is viewed as a series of simple Bernoulli trials (Smith 1987) with two possible outcomes. Given the persistence of meteorological conditions, the probability of an outcome is influenced by the previous outcome. Generally, this dependency is modelled using a first order Markov chain (Conejo, et al. 2001). Figure 2 show all possible combinations of the wet/dry conditions in two consecutive days. Only estimates of probabilities in the two shaded boxes are needed, as the probability of the other outcome is the statistical complement.

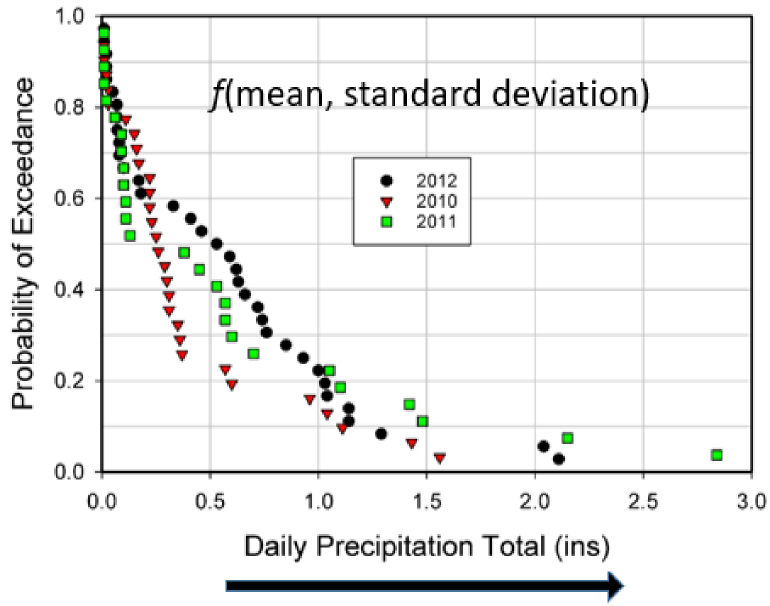

Figure 3. Daily precipitation total in inches (x-axis) versus the probability of exceedance (y-axis) for the winters of 2010-2012. Defining magnitude of daily precipitation.

How much precipitation falls on a rainy day, is generally represented by an exponential-type probability distribution as shown in Figure 3. A generalized Pareto distribution is commonly used for this purpose (Lennartson et al., 2008) and its parameters can be estimated by the method of moments from the sample mean ($\hat{\mu}$) and standard deviation ($\hat{\sigma}$) (Rosbjerg, et al., 1992) as:

$$\hat{a} = \frac{1}{2}\hat{\mu}\left(\frac{\hat{\mu}^2}{\hat{\sigma}^2} + 1\right) \quad (1)$$

$$\hat{k} = \frac{1}{2}\left(\frac{\hat{\mu}^2}{\hat{\sigma}^2} - 1\right) \quad (2)$$

Variable	Notation	Computation
Wet day	W	
Dry day	D	
Number of days in winter	n	
Number of wet days	n_W	
Number of dry days	n_D	
Proportion of days wet		n_W/n
Number of occasions that a wet day follows a wet day	n_{WW}	
Number of occasions that a dry day follows a dry day	n_{DD}	
Transition probability of a wet day to wet day	W|W	n_{WW} / n_W
Transition probability of a dry day to dry day	D|D	n_{DD} / n_D
Mean daily precipitation	$\hat{\mu}$	$\frac{1}{n}\sum_{i}^{n} P_i \;\forall\, P_i > 0$
Standard deviation of daily precipitation	$\hat{\sigma}$	$\sqrt{\{\left(\frac{1}{n}\right)\sum_{i}^{n}(P_{i-}\,\hat{\mu})^2\}} \;\forall\, P_i > 0$

Table 1. Table of definitions for daily precipitation variables, for the winter season, examined in the research including; a) the proportion total number of days with precipitation, b) the probability of a wet day following a wet day (number of occasions that consecutive wet days occur/the number of wet days), c) the probability of a dry day following a dry day (number of occasions that consecutive dry days occur/the number of dry days), d) the average depth of precipitation on wet days, and c) the standard deviation of the depth of precipitation on wet days.

Variables extracted annually during the four months treated as winter (December to March inclusive), are defined in Table 1. Years are identified by the calendar year into which December falls, for example, the winter from December 2012 to March of 2013 is identified as 2012, a convention used in the ENSO classification. Winters with any missing records are excluded from further analysis. Each winter the number of occurrences of consecutive days of similar "states" (dry or wet) are compared to the total number of transitions (the total number o days-1) and the proportion days experiencing measurable precipitation are recorded. Knowledge of these transitions also determines the likely lengths of the number of consecutive wet days (wet spells) or dry days (dry spells). Observed lengths of these spells each winter are also extracted, spells which have no defined start or end within the four months are excluded. Whenever precipitation occurs, the daily total is extracted and at the end of each winter their mean and standard deviation computed. All subsequent analyses are carried out in Microsoft EXCEL.

Methods

If the variables in each subpopulation (warm, cold and neutral) are approximately normally distributed, then the standard parametric F- and t-tests can be used to determine significant differences in their variances and means between the three phases. Test for variances must be considered first to determine the correct form of the t-test. Empirical cumulative probabilities, $P(x \leq X)$, are estimated for each of the seven variables in the reported phases of ENSO, using the simple Weibull plotting position (Cunnane, 1978) of

$$P(x \leq X) = \text{Rank of } X/(n+1) \tag{3}$$

where the n observations within each ENSO phase are sorted and ranked (smallest = 1, largest = n). Normal distributions possessing the same mean and variance as the observed data are created and the Kolmogorov-Smirnov (K-S) goodness of fit test applied (Masereka, et al., 2018). The null hypothesis of no significant difference between the observed cumulative probabilities and the fitted normal distributions, is applied to all 21 (seven variables defined in Table 1, three ENSO phases) variables/subpopulations. Tests are carried out at the 0.20 level of significance (lowest tabulated values) in order to reduce the probability of making a Type-II error in hypothesis testing.

To cover the possibility that data are not normally distributed, comparisons of the values of observed variables in each ENSO phase are performed via the hypergeometric distribution (Grimm et al., 2000). Data from all years are sorted regardless of ENSO phase. A count is kept of the number of years of each ENSO phase falling in the upper (lower) tercile of those sorted data. Under the null hypothesis that ENSO has no role in determining annual values, it would be expected that one third of all years of a particular phase would appear in each tercile (e.g. on average one would expected ten of the 30 observations of neutral years to fall in any tercile). Under the null condition, the probability of finding any number of years, k, of the specified ENSO phase in a tercile is defined by the hypergeometric distribution.

$$P(X=k) = \frac{\binom{K}{k}\binom{N-K}{n-k}}{\binom{N}{n}} \tag{4}$$

Where N is the total number of all observations (63), K is the number of those observations that possess the property of interest (years in each ENSO subpopulation) and n is the size of the sample taken (21 in each tercile). From this distribution, probabilities of unusually large or small outcomes can be defined and compared to predefined critical values. Tests throughout are carried out at the 0.05 level unless otherwise stated.

Results

The K-S test failed to reject the null hypothesis in any combination of subpopulations/variables, indicating that the assumption of normality is reasonable. There is insufficient evidence in any case to reject the null hypothesis of no significant differences in variances despite some visual differences (e.g. Figure 4) - probably the result of the comparatively small sample sizes of warm and cold phase ENSO years. On that basis, a two-tailed, equal variance, t-test is used to compare means.

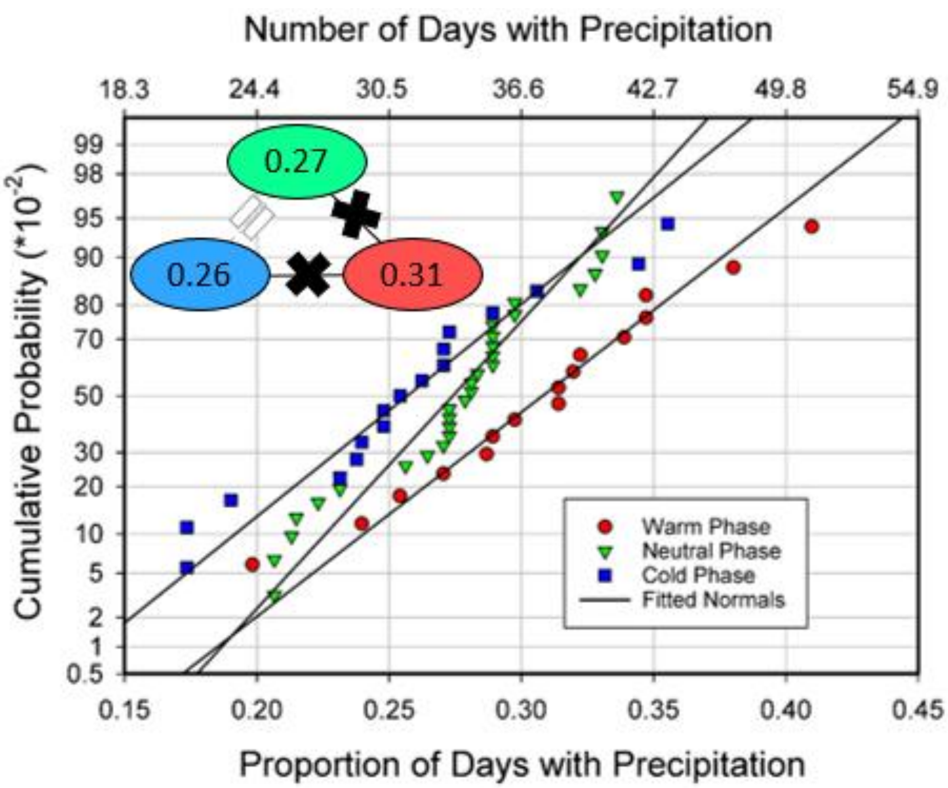

Figure 4. Probability distributions of the proportion of days with precipitation (bottom axis) and number of days with precipitation (top axis) under various phases of ENSO. Figures inside the ovals report the mean of the proportion of days in each phase. An equal sign on the lines connecting ovals indicates no significant difference in means and a black “X” indicates significant difference.

Table 2 displays estimated means of the seven variables under each phase of ENSO. These confirm the widely-made observation that winters are wetter during warm phases and drier in cold phases, however they provide valuable insights into the way in which these seasonal totals are derived in terms of the frequency and magnitude of daily precipitation, and their sequencing, at a temporal scale more appropriate for many management practices. The mean proportion of days with measurable precipitation, a coarse measure of the frequency of events, rises from 0.257(25.7% of winter days) during cold phase to 0.308 (30.8%) in warm phase. The important sequencing of consecutive days with similar states (precipitation/no precipitation) characterized in weather generators by D|D and W|W transition probabilities, reveals an interesting nuance describing the nature of this change in frequency. Mean D|D transitions vary little (0.028, or about 3.6% of undifferentiated D|D values) between the phases, with the highest value (0.776), as expected occurring in the drier cold phase and the lowest (0.748) in the wetter warm phase. Mean W|W transitions however display greater differences in terms of both absolute values (0.092) and percentages of undifferentiated values (23.1%). Suggesting that, in physical terms, lengths of consecutive dry days (dry spells), probably change little between phases, while consecutive days with measurable precipitation (wet spells) are more likely be responsive of ENSO phase. Empirical observations of the mean lengths of dry (4.15 days in cold phase, and 3.78 days in warm) and wet spells (1.51 days in cold and 1.82 days in warm) initially seem not to support this. However, once the changes (0.37 and 0.31 days respectively) are expressed as percentages of the undifferentiated means, the proportionate changes become clear (9% for dry spells and 19% for wet).

Variable	Cold Phase	Neutral Phase	Warm Phase
Proportion of days	0.257	0.274	0.308
D|D Probability	0.776	0.772	0.748
W|W Probability	0.347	0.398	0.439
Mean Total (in)	0.498	0.554	0.646
St.Dev. Total (in)	0.641	0.751	0.838
Coeff. of Variation(%)	1.29	1.36	1.30
Mean Dry Spell (dy)	4.15	4.00	3.78
Mean Wet Spell (dy)	1.51	1.62	1.82

Table 2. Estimated mean value of parameters of daily precipitation under the three phases of ENSO.

Not only do the daily frequency characteristics of the precipitation change, but so do those of the magnitude of daily precipitation totals. Mean daily totals increase from 0.498” (cold phase) to 0.646” (warm phase), a 27% increase. Perhaps of greater significance in terms of risks associated with excess precipitation (flooding, erosion, sedimentation), is that this increase in means is accompanied by an increase in the average value of the standard deviation of precipitation totals (0.641” in cold phase and 0.838” in warm) in a season. As precipitation can only assume positive values, this increase in the average value of the standard deviation (0.197” or 26% of undifferentiated) can only be accommodated by increases in the upper tail of the distribution – the larger daily totals. The coefficient of variation (standard deviation/mean) remains fairly constant across phases. The fact that they are all greater than unity implies that a distribution with a “heavier tail” than an exponential, like the Generalized Pareto, would be required

Table 3 summarizes the statistical significance of the comparisons of means and supports the notion that, with the exception of D|D transitions, the parameters entered into weather generators, and the resultant probabilities of daily winter precipitation should change with the state of ENSO. The contrast between warm and neutral phases is less marked and, statistically, cold and neutral phases are almost indistinct.

Given the small sub-sample sizes of warm and cold phases and the very conservative nature of the K-S test, the non-parametric hypergeometric is used to validate the conclusions drawn about differences in values for a weather generator between ENSO phases.

Variable / **Compare**	**Prop.**	**D|D**	**W|W**	**Mean**	**St. Dev.**	**Dry Spells**	**Wet Spells**
Warm/Cold	W*		W*	W*	W	C	W
Warm/Neutral	W*	N		W*		N*	W*
Cold/Neutral			N				

Table 3. Summary of the statistical significance of comparisons of means of each variable under various phases of ENSO. Empty cell indicates no significant difference. Letters identify the phase of ENSO – **W**arm (n= 16), **N**eutral (n=30), **C**old (n=17) - generating the larger mean at 0.10 level. Asterisks show significant differences at the 0.05 level.

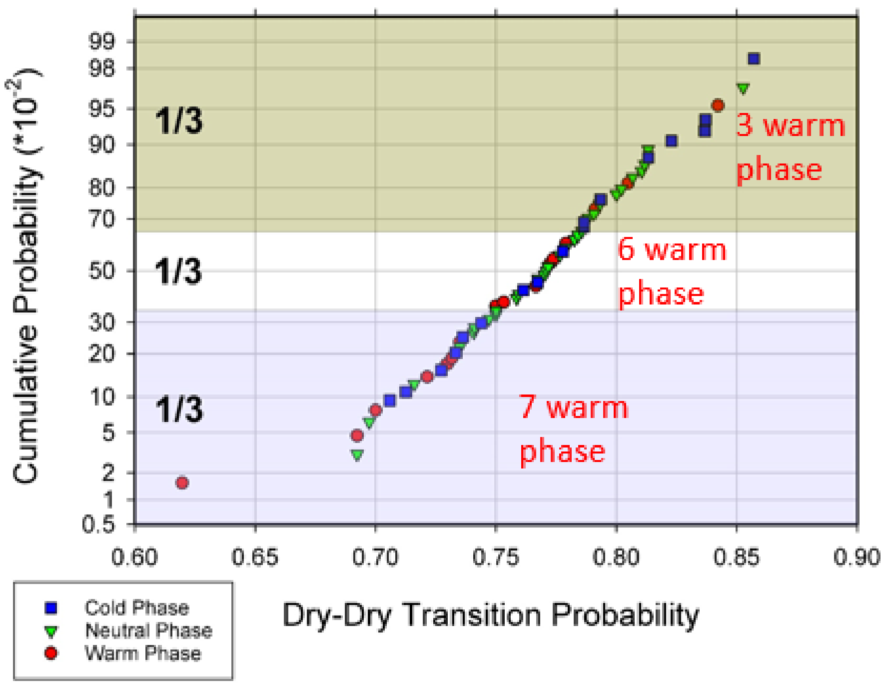

Figure 5. Empirical distribution of all annual estimates of D|D transition probabilities, identified by ENSO phase. Data are divided into three groups (terciles) of equal membership. As an example of the test of the hypergeometric probability distribution, the number of occasions that warm phase years fall in each tercile is recorded.

Figure 5 plots all 63 annual estimates of D|D transition probabilities, identified by ENSO phase. Data are divided into terciles and particular attention is paid to the 21 observations with the largest D|D transition probabilities (upper tercile) and the 21 with the smallest (lower tercile). The former would be years likely to experience the longest dry spells while the latter would likely experience the shortest. In total sixteen years are classified as warm phase. If estimates of D|D are independent of phase, then roughly five warm phase years would be expected in each tercile. As it is, only three warm phase years fall in the upper tercile and seven in the lower. The hypergeometric distribution permits calculation of the probabilities of these outcomes under the null hypothesis of randomness. In neither case are the chances of the observed values sufficiently large or small to permit rejection of randomness at either the 0.10 or 0.05 levels, supporting the result in the upper row of Table 3 of no significant difference in the mean values of D|D between warm and cold phases.

Given a particular phase of ENSO, the observed numbers of years falling in either the upper, or lower, tercile classes of each variable can be greater than, less than, or not significantly different from, that expected at random. Figures 7 and 8 summarize the nature of the relationships (greater above line, less below line) for upper and lower terciles of the five parameters directly related the weather generator. The proportion of days with precipitation during warm phase occurs significantly more frequently in the upper tercile than random, as do values of the mean and standard deviation of precipitation - but at only the 0.10 level.

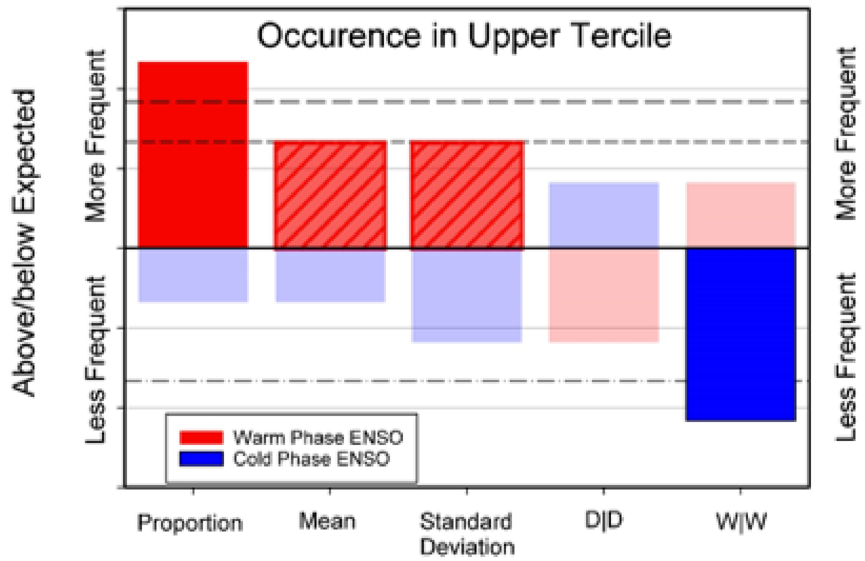

Figure 6. Results of the application of the hypergeometric distribution to frequencies with which the observed values of parameters of the weather generator fall within the upper tercile of all values. Heavy colors indicate significance and hashing at the 0.10 level.

Values of W|W transitions during cold phase years fall significantly fewer times in the upper tercile and D|D probabilities show no tendencies. These observations are consistent with previous results, of 1) more days with precipitation and larger totals during warm phases, and 2) lower probabilities of consecutive wet days during cold phases.

Cold phase years appear more prominently in the analysis of frequencies with which estimates fall in the lower tercile of all parameter values (Figure 7). All parameters, except for D|D, occur more often at the 0.10 level. The tendency for larger mean daily precipitation totals in warm phase years is illustrated by significantly fewer estimates of this variable within the lower tercile.

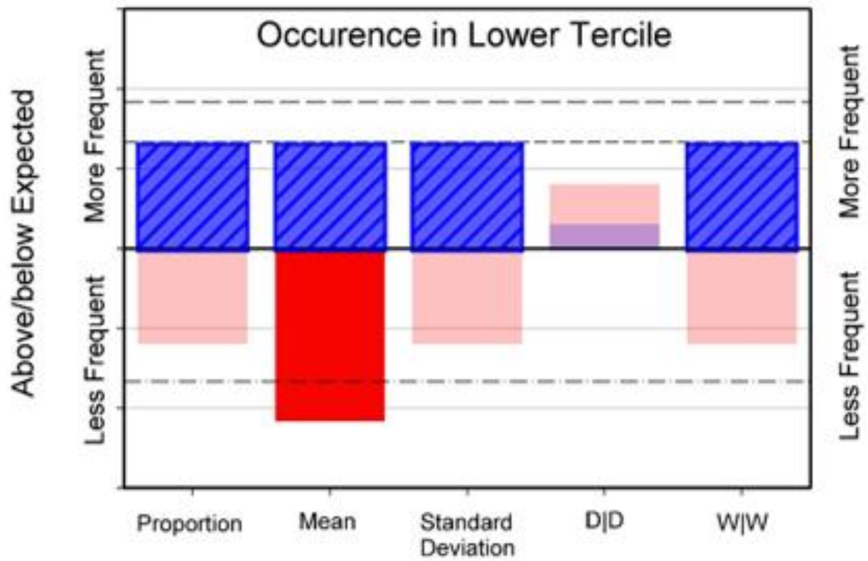

Figure 7**.** Results of the application of the hypergeometric distribution to frequencies with which the observed values of parameters of the weather generator fall within the lower tercile of all values. Heavy colors indicate significance and hashing at the 0.10 level.

Discussion

More complex versions of weather generators which use higher orders of Markov chain (Harrison and Waylen, 2000) and different probability distributions exist (Hanson and Vogel, 2008), but the approach and types of parameters remain basically the same as those shown here. This research has focused on changes in the values of parameters necessary to operationalize weather generators under current climate variability, rather than the exact forms of models to be used.

The goodness of fit test of the assumption of normality, suffers from the same issues that many such tests which are generally established to minimize the chance of making a Type I error. Visually, plots such as Figures 4 and 5 support the statistical conclusions and a small degree of non-normality does not preclude the use of the parametric tests, it only reduces the likely significance of the results. Application of the non-parametric hypergeometric distribution test bolsters the findings. Terciles are used as categories ("above normal", "normal" and "below normal") as they are used widely in climate forecasting (see for example, https://iri.columbia.edu/our-expertise/climate/forecasts/seasonal-climate-forecasts/).

Although the focus is on the collective set of parameters used to describe the variables in weather generators, knowledge of the probability distribution of each individual variable is also of value. For instance, Figure 8 displays the probability of W|W transitions separated by ENSO phase. The "average" estimate of this variable's probability over all 63 years is about 0.4. The probability of experiencing this value or less in a warm phase year is about 0.30, rising to over 0.70 in cool phases. Likewise, choosing a measure of relative "rareness" of a particular value, such as a roughly 20 year return period excess (0.95 cumulative probability) or deficit (0.05 cumulative probability), estimated W|W values range from 0.46 (cold) to 0.55(warm) , and 0.20 (cold) to 0.31(warm), respectively. Knowledge of the normality of these variables, therefore, conveys a great deal more valuable practical information than just a simple table of the means and standard deviations.

While these are only point measurements made at Tallahassee, they are based on the longest and most complete daily record in the area of the state most impacted by ENSO and therefore provide the largest sub-population sizes upon which to complete tests. Given the regional nature of seasonal frontal precipitation, the lack of major topographic barriers and the well documented regional extent of ENSO impacts, it is reasonable to assume that similar changes will be experienced regionally, even if the exact sizes of those changes vary from location to location.

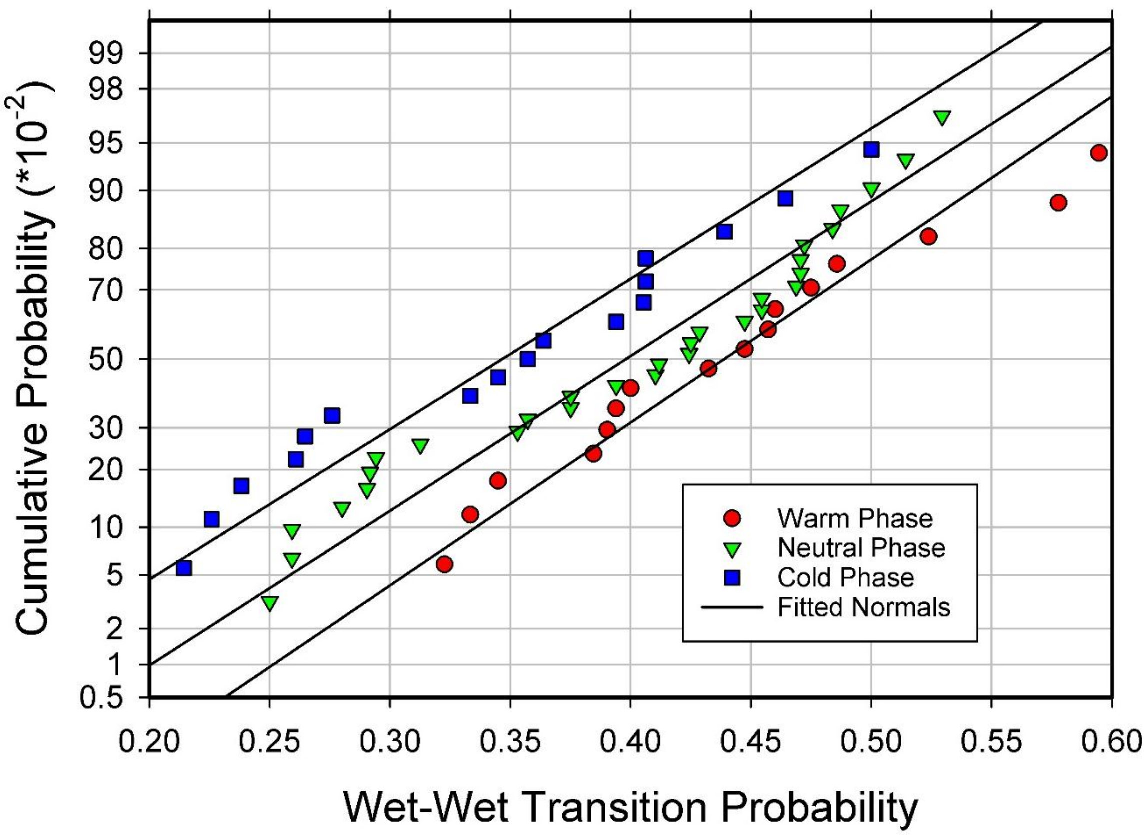

Figure 8. Probability distributions of the estimated W|W transition probability under various phases of ENSO.

Conclusions

This work disaggregates to the daily scale the well-known impacts of ENSO in the panhandle, north and central Florida on winter precipitation totals. In doing so it highlights comparative changes in both the frequency (transition probabilities, proportion of days with measurable precipitation), and magnitude (mean and standard deviation of daily totals) of the precipitation process, as well as the risks of excessive wet or dry spells. Given the extensive use of weather generators in numerous practical planning and forecasting applications, these changes can be important to decision-making in local forestry, agricultural, tourism and fisheries activities. In particular, if a warm phase event is forecast as opposed to a cold phase, the following changes might be anticipated: a) an increase in the proportion of winter days with measurable precipitation, b) an increase in the probability of wet to wet transitions, c) an increase in the mean length of wet spells, d) a decrease in the mean length of dry spells, and e) a proportionate (coefficient of variation) increase in both the mean and standard deviation of daily precipitation totals. When comparing warm and neutral phases, contrasts are similar, but less frequently statistically significant, with the exception that dry-to-dry transitions are shorter in warm phases. Few statistically significant distinctions exist between cold and neutral phases.

Works Cited

Bovy, B., Braun, J. and Demoulin, A., 2016. A new numerical framework for simulating the control of weather and climate on the evolution of soil-mantled hillslopes. *Geomorphology*, *263*, pp.99-112.

Cai, W., Borlace, S., Lengaigne, M., Van Rensch, P., Collins, M., Vecchi, G., Timmermann, A., Santoso, A., McPhaden, M.J., Wu, L. and England, M.H., 2014. Increasing frequency of extreme El Niño events due to greenhouse warming. *Nature climate change*, *4*(2), p.111-116.

Cai, W., Wang, G., Dewitte, B., Wu, L., Santoso, A., Takahashi, K., Yang, Y., Carréric, A. and McPhaden, M.J., 2018. Increased variability of eastern Pacific El Niño under greenhouse warming. *Nature*, *564*(7735), p.201.

Conejo, S., Morata, A., and Valero, F., 2001. First order Markov chain model and rainfall sequences in several stations of Spain. *Detecting and Modelling Regional Climate Change,* 417-428.

Cunnane, C., 1978. Unbiased plotting positions—a review. *Journal of Hydrology*, *37*(3-4), pp.205-222.

Elliot, W.J., Miller, M.E. and Enstice, N., 2016. Targeting forest management through fire and erosion modelling. *International Journal of Wildland Fire*, *25*(8), pp.876-887.

Florida Climate Center, Florida State University. Downloadable Data. Retrieved from https://climatecenter.fsu.edu/climate-data-access-tools/downloadable-data

Grimm, A.M., Barros, V.R. and Doyle, M.E., 2000. Climate variability in southern South America associated with El Niño and La Niña events. *Journal of climate*, *13*(1), pp.35-58.

Hanson, L.S. and Vogel, R., 2008. The probability distribution of daily rainfall in the United States. In *World Environmental and Water Resources Congress 2008: Ahupua'A* (pp. 1-10).

Harrison, M. and Waylen, P., 2000. A note concerning the proper choice for Markov model order for daily precipitation in the humid tropics: A case study in Costa Rica. *International Journal of Climatology*, *20*(14), pp.1861-1872.

Herman, J.D., Zeff, H.B., Lamontagne, J.R., Reed, P.M. and Characklis, G.W., 2016. Synthetic drought scenario generation to support bottom-up water supply vulnerability assessments. *Journal of Water Resources Planning and Management*, *142*(11), p.04016050.

Jones, J.W., 1993. Decision support systems for agricultural development. In *Systems Approaches for Agricultural Development* (pp. 459-471). Springer, Dordrecht.

Kinnell, P.I.A., 2019. CLIGEN as a weather generator for RUSLE2. *CATENA*, *172*, pp.877-880.

Lennartsson, J., Baxevani, A. and Chen, D., 2008. Modelling precipitation in Sweden using multiple step Markov chains and a composite model. *Journal of Hydrology*, *363*(1-4), pp.42-59.

Maleski, J.J. and Martinez, C.J., 2018. Coupled impacts of ENSO AMO and PDO on temperature and precipitation in the Alabama–Coosa–Tallapoosa and Apalachicola–Chattahoochee–Flint river basins. *International Journal of Climatology*, *38*, pp.e717-e728.

Masereka, E. M., Ochieng, G. M., and Snyman, J., 2018. Statistical analysis of annual maximum daily rainfall for Nelspruit and its environs. *Jàmbá: Journal of Disaster Risk Studies, 10*(1). doi:10.4102/jamba.v10i1.499

Rosbjerg, D., Madsen, H. and Rasmussen, P.F., 1992. Prediction in partial duration series with generalized Pareto-distributed exceedances. *Water Resources Research*, *28*(11), pp.3001-3010.

Schmidt, N., Lipp, E.K., Rose, J.B. and Luther, M.E., 2001. ENSO influences on seasonal rainfall and river discharge in Florida. *Journal of Climate*, *14*(4), pp.615-628.

Smith, J. A., 1987. Statistical modeling of daily rainfall occurrences. *Water Resources Research, 23*(5), 885-893.

Sparks, N.J., Hardwick, S.R., Schmid, M. and Toumi, R., 2018. IMAGE: a multivariate multi-site stochastic weather generator for European weather and climate. *Stochastic Environmental Research and Risk Assessment*, *32*(3), pp.771-784.

Sunde, M.G., He, H.S., Hubbart, J.A. and Urban, M.A., 2017. Integrating downscaled CMIP5 data with a physically based hydrologic model to estimate potential climate change impacts on streamflow processes in a mixed-use watershed. *Hydrological Processes*, *31*(9), pp.1790-1803.

Wang, H. and Asefa, T., 2018. Impact of different types of ENSO conditions on seasonal precipitation and streamflow in the Southeastern United States. *International Journal of Climatology*, *38*(3), pp.1438-1451.

Wilks, D.S. and Wilby, R.L., 1999. The weather generation game: a review of stochastic weather models. *Progress in Physical Geography*, *23*(3), pp.329-357.

Web Sites Cited

https://iridl.ldeo.columbia.edu/maproom/ENSO/ENSO_Info.html/ “What is ENSO?” International Research Institute for Climate and Society, Earth Institute, Columbia University, NY. Last accessed July 2019.

https://www.coaps.fsu.edu/jma/ ENSO Index According to JMA SSTA (1868-present). Center for Ocean Atmosphere Prediction Studies, Florida State University, Tallahassee, FL. Last accessed July 2019.

http://climatecenter.fsu.edu/jumi/climate_visualization/Climate_Data.php. Climate Center, Florida State University, Tallahassee, FL. Last accessed July 2019.

https://iri.columbia.edu/our-expertise/climate/forecasts/seasonal-climate-forecasts/. International Research Institute for Climate and Society, Earth Institute, Columbia University, NY. Last accessed July 2019.